Neutron Spectra and Dose Equivalent Inside Nuclear Power Reactor Containment

Prepared by J. M. Aldrich

Pacific Northwest Laboratory
Operated by
Battelle Memorial Institute

Neutron Spectra and Dose Equivalent Inside Nuclear Power Reactor Containment

Prepared by
J. M. Aldrich

Pacific Northwest Laboratory
Richland, WA 99352

ABSTRACT

This study was conducted to determine absorbed dose, dose-equivalent rates, and neutron spectra inside containment at nuclear power plants. We gratefully acknowledge funding support by the Nuclear Regulatory Commission.

The purpose of this study is:

1) measure dose-equivalent rates with various commercial types of rem meters, such as the Snoopy and Rascal, and neutron absorbed dose rates with a tissue-equivalent proportional counter

2) determine neutron spectra using the multisphere or Bonner sphere technique and a helium-3 spectrometer

3) compare several types of personnel neutron dosimeter responses such as NTA film, polycarbonates, TLD albedo, and a recently introduced proton recoil track etch dosimeter, and CR-39.

These measurements were made inside containments of pressurized water reactors (PWRs) and outside containment penetrations of boiling water reactors (BWRs) operating at full power. The neutron spectral information, absorbed dose, and dose-equivalent measurements are needed for proper interpretation of instrument and personnel dosimeter responses.

ACKNOWLEDGMENTS

SUMMARY

Neutron dose equivalent rates and spectra were measured inside containment of two pressurized water reactors operating at full power. Dose equivalent rates were measured by a tissue equivalent proportional counter and the neutron spectra by a multisphere (Bonner sphere) spectrometer.

There were significant variations in dose equivalent rates and spectra among various locations on the reactor operating deck, dependent on the amount of neutron streaming. Spectral results revealed "soft" neutron spectra with almost all of the neutrons having energies below 1 MeV.

Measured dose equivalent rates ranged from 0.05 to 3080 mrem/hr and the average neutron energies ranged from 0.9 to 90 keV. After significant neutron shielding modification at one reactor, the dose equivalent rates were reduced by a factor of about 30 and the average neutron energies were reduced by a factor of 1.5.

CONTENTS

FIGURES

TABLES

NEUTRON SPECTRA AND DOSE EQUIVALENT INSIDE
NUCLEAR POWER REACTOR CONTAINMENT

INTRODUCTION

Throughout the history of commercial nuclear power reactors in the United States, the philosophy has been to overdesign and overbuild to ensure safety. In recent years, in particular, increased demands have been placed on the nuclear industry to provide additional protection for the public and operations personnel. Moreover, recent studies by Rossi and Mays (1978) suggest that quality factors for fast neutrons should be increased by approximately a factor of 10. The quality factor is a value based on linear energy transfer (LET), by which the absorbed dose is multiplied to obtain the dose equivalent.

The energy imparted to tissue has been adopted as a principal physical basis of quantitative correlation between irradiation and biological effect. The energy per unit mass that is imparted to matter by ionizing radiation is the absorbed dose. Its special unit is the rad (100 ergs/gm). Dose equivalent is based on the assumption that differences in biological effects of radiations are related to differences in linear energy transfer of the charged particles that deliver the absorbed dose. Consequently, the limits of radiation exposure of personnel are expressed in terms of the dose equivalent, which has the special unit rem. The quality factor is specific as a factor of linear energy transfer and has a numerical value of 1 of x- and gamma-rays. In all practical cases involving more densely ionizing particles, such as neutron recoils, the values of quality factor change for various neutron energies. Hence, the dose equivalent is equal to the absorbed dose times the applicable quality factor (Brackenbush, Endres, and Faust 1973).

The impact of Rossi's studies could result in more stringent operational controls which in effect reduce the allowable absorbed dose from neutrons. This potential reduction in allowable neutron exposure has motivated the nuclear industry to strive for better shielding, improved neutron monitoring instrumentation, and more accurate personnel neutron dosimeters.

1

In addition, the nuclear industry has instituted an operational program known as "As Low As Reasonably Achievable" (ALARA), which, simply stated, means no single individual should receive any more exposure than is absolutely necessary to perform a job. Thus, in many cases, it is necessary to measure accurately relatively low dose-equivalent rates from neutrons (0-50 mrem/hr). The tedious dosimetry method by which this is accomplished depends on knowledge of the neutron-to-gamma dose-equivalent rate ratio at every work location inside reactor containment, or by ad hoc measurements with portable instruments which are used to establish the stay time. Stay time is the amount of time permitted in a specific dose-equivalent rate area such that a predetermined dose equivalent will not be exceeded. Minor maintenance, valve adjustments, and semi-routine surveys in containment during full power operations are some of the situations requiring this type of dosimeter.

There have been few systematic investigations of the stray neutron radiation fields to which workers and instruments inside containments of nuclear power reactors may be exposed (Hajnal 1979; Hankins and Griffith 1978). Hence, neutron spectra and dose-equivalent rates to workers at power reactors are not well known. Recent concern about personnel exposure to neutrons, personnel neutron dosimeter response, and in particular the concept of ALARA, has motivated the development of better measurements and data. This new data will be used to evaluate the distribution of dose equivalents to workers and to determine operational levels of exposure.

Determination of neutron dose or dose-equivalent values and their distributions with neutron energy in the presence of significant gamma-ray levels inside the containments of pressurized water reactors (PWR's) with available instrumentation is much more difficult than similar measurements outside containments. The unpleasant, if not hostile conditions of high ambient temperature, humidity, possible airborne radioactivity and surface contamination complicate the required spectrometric measurements.

The purposes of this study are 1) to measure the neutron spectra and dose equivalents inside containment of two PWR's, and 2) to interpret this data with respect to design and shielding differences. These in-containment measurements are the first to be used for design and shielding comparisons

2

between individual reactors. The reactors were operating at approximately 100% power for the duration of the measurements.

For this study, a multisphere spectrometer system, as described by Awschalom (1966), and a tissue equivalent proportional counter detector (TEPC) were used (Smith et al. 1978). The multisphere system was originally developed in the late 1950's by Bramblett, Ewing and Bonner (1960) who made limited application of the system around reactors. This system is commonly known as the "Bonner spheres".

Analysis of the multisphere and TEPC data is accomplished with two separate computer programs, LOUHI-78 and TEPC, respectively (Routti, Sandberg 1978; Brackenbush, Endres, and Faust 1979). The analyzed results from these two programs are correlated with specific locations inside containment in which operating plant personnel are semi-routinely exposed to various neutron radiation fields.

Although the multisphere spectrometer system has a relatively low resolution, its wide energy range, especially at the lower end (0-50 keV), is very useful for spectral measurements in reactor containments. When used in conjunction with the LOUHI computer code, several other parameters including the dose-equivalent rate can be calculated. Dose-equivalent rates obtained with the multisphere system were found to agree within ±20% of values obtained with a calibration source (Hankins and Griffith 1978).

The multisphere, as its name implies, uses several spheres for a single analysis whereas the TEPC requires but a single measurement. The TEPC is designed to measure absorbed dose with an uncertainity of ±10% (Brackenbush, Endres and Faust 1973) using a gas-filled tissue equivalent chamber. The TEPC results are also used for the determination of the quality factor (Q) in the unknown neutron spectrum.

The nuclear power generating stations examined in this study are identified as Site F and Site I to prevent identification in accordance with the agreement between the Nuclear Regulatory Commission and the licensee regarding these measurements. Both reactors have the same pressurized water nuclear steam supply system with Site I producing 934 MWe and

3

Site F 100 MWe. The major difference between the two units is the containment structural design and associated shielding, each having been designed by different architect-engineers. The differences in neutron spectra and dose equivalents are related to these design configurations and characteristics.

Two trips were made to Site I in order to obtain measurements involving a major shielding change. Between the trips a new neutron attenuating material, a silicon-based elastomer impregnated with boron, was installed around the inlet and outlet nozzles and around the reactor vessel. The effects of these shielding changes on the neutron spectra and dose equivalent rates are evaluated with respect to personnel protection. This is the first time spectrometer and dose equivalent rate measurements have been made before and after a significant shielding modification.

MATERIALS AND METHODS

The two measurement systems selected for use in this study were the multisphere spectrometer system (Awschalom 1966) and a tissue equivalent proportional counter system (TEPC) (Smith et al. 1978). Multispheres are the best available commercial system for measuring intermediate neutron energy spectra and are also capable of detecting neutrons in the thermal to 50 keV energy range. When the multisphere system is used with a spectrum unfolding code such as LOUHI (Routti and Sandberg 1978), the average neutron energy, dose-equivalent rate, total flux, and graphical plots of differential flux versus energy, flux per unit lethargy versus energy, and flux versus energy can be obtained. For the purposes of this study, graphical plots of differential flux versus energy and flux per unit lethargy versus energy will not be used. The multisphere system is also the best system available for determining the intermediate neutron energy inside reactor containments in the 1 keV and 1 MeV range (Griffith and Fisher 1976). The research-oriented TEPC system measures total absorbed dose and the TEPC computer code calculates the dose distribution as a function of event size. The TEPC computer code also calculates a quality factor by using the Rossi analysis (1968) and several approximations derived by Brackenbush, Endres and Faust (1973).

MULTISPHERE SPECTROMETER SYSTEM

The multisphere neutron system and specific instrument settings used in this work are shown in block diagram in Figure 1. The detector is a cylindrical ^{6}LiI(Eu) scintaillation crystal, 1.27 cm in diameter by 1.27 cm long, optically coupled to a photomultiplier tube (PMT) through a 20.32 cm light pipe. The detector and its intergral components were hermatically sealed in an aluminum tube with walls 0.16-cm thick. The PMT is surrounded by a brass sleeve for protection and support for cable connectors. A single cable carries both the high voltage and output signals, connecting the detector to a preamplifier which decouples the signals and feeds them into the multichannel analyzer (MCA). The analyzer has three built-in systems as
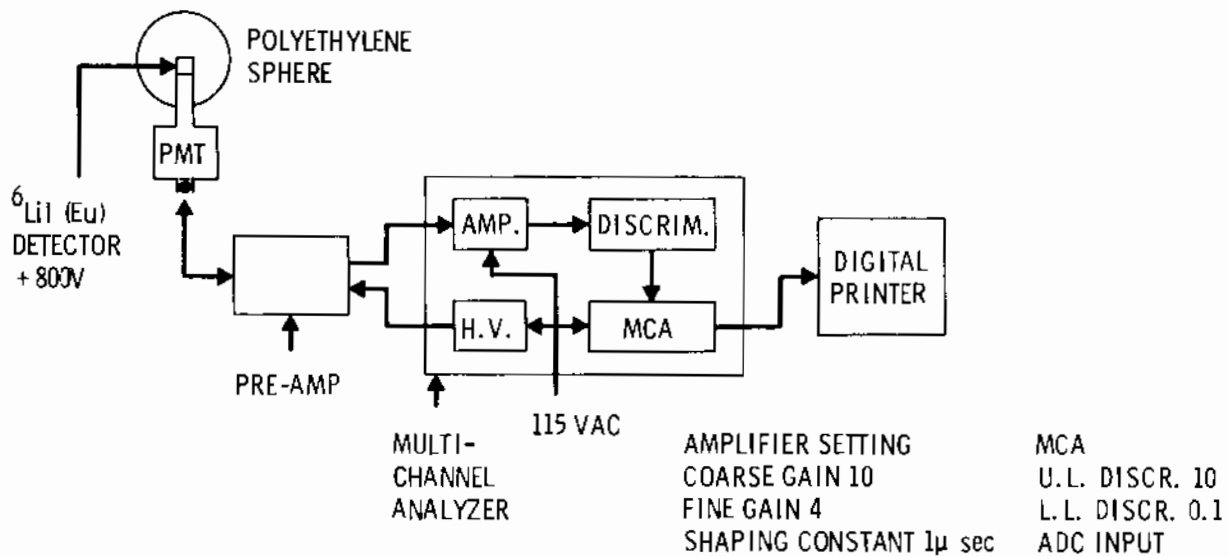
FIGURE 1. Block Diagram of the Multisphere System.

integral parts: amplifier, high voltage power supply, and discriminators. The unanalyzed data is directly obtained from the MCA and fed to a printer for hard copy.

The neutron detection mechanism exhibited by the ^{6}LiI(Eu) cyrstal is the ^{6}Li(n,α) ^{3}H reaction for thermal neutrons. This reaction is exoergic and deposits an equivalent electron energy of 4.8 MeV in the scintillator, producing a distinct peak in the pulse height spectrum shown in the MCA. Interpretation of the full width peak area is defined from the point at which the n,α reaction begins to be detected, to the point in which the peak rejoins background interactions. There are no other competing peaks in the spectrum. An exponential background continuum is subtracted from the full width peak area. The exponential or log background subtraction technique is simply the subtraction of background from the region of interest when the unanalyzed data is plotted on a log scale. Background contribution to the region of interest or thermal peak has been shown to be logarithmic through several experiments. A supporting experiment is a comparison between ^{6}LiI and ^{7}LiI cystals, which have exactly the same response to gammas. However, ^{6}Li has a very high cross-section for the (n,α) reaction with

6

thermal neutrons (945 barns) (Hughes and Harvey 1955). Thus, when a ^{7}LiI gamma spectrum is superimposed over the ^{6}LiI gamma plus neutron spectrum they are identical except at the thermal neutron peak. The background under the peak is determined from the ^{7}LiI spectrum, and is subtracted from the ^{6}LiI thermal neutron peak by a technique known as log background subtraction, so named because the background counts vary logarithmically as a function of channel number. The same results are obtained when a ^{6}LiI crystal is exposed only to gamma and then to a mixed gamma plus neutron field and the two spectra superimposed on each other and the log background subtraction performed.

Unanalyzed data for the neutron energy spectrum is obtained by taking counts with the scintillation crystal unshielded (bare), with the crystal in a cadmium shell 0.051 cm thick, and with the crystal moderated by spheres of high density polyethylene 7.6, 12.7, 20.3, 25.5, and 30.5 cm in diameter. The fast neutron response of this system increases with sphere size because the larger polyethylene spheres remove low energy neutrons by scattering and absorption but moderate the fast neutrons to lower energies where they are then detected with a greater probability by the ^{6}LiI(Eu) scintillator. Cadmium shells placed around the 7.6 and 12.7 cm spheres suppress response to external thermal neutron fields which improves the systems' ability to detect moderated fast neutrons above the cadmium cutoff (0.4 eV)(Hankins and Griffith 1978).

Using the responses from the seven detector configurations (bare, cadmium covered, 7.6, 12.7, 20.3, 25.5, and 30.5 cm moderators), the spectrum is unfolded with the aid of the LOUHI computer code. LOUHI is a FORTRAN program written to solve Fredholm integral equations of the first kind by using a generalized least-squares procedure with non-negative solutions. With LOUHI, the spectral solution is not dependent on the choice of initial approximation. By calculating the flux in a particular party of the spectrum, based on the response of the 12.7 cm sphere, the 26th energy bin or upper limit of the energy range over which the spectrum is to be calculated can be "tied" to that point (Hankins and Griffith 1978). For this study, this feature is used to place the high energy bin at a realistic value which

reflects the general lack of source neutrons above 15 MeV (Hajnal 1979; Hankins and Griffith 1978).

Considerations were given to error amplifications introduced through overlapping responses between different sizes of spheres (Griffith et al. 1977; Zaidins, Martin, and Edwards 1978; Routti 1969). Amplified errors arise from the errors associated with each sphere response. The sphere response errors are increased at each iteration so that amplification occurs as the code unfolds the spectrum through several iterations. The mathematics of LOUHI, when compared to the mathematics of error calculations developed for foil activation unfolding codes (Robkin 1968), indicate similar inherent error problems. LOUHI minimizes these errors by weighting functions and varying the emphasis of each detector response. Neutron energy response functions calculated by Sanna (1973) are used as input for the unfolding process. Sanna's calculations are based on one-dimensional spherical geometries and were verified empirically in the energy range 100 keV to 20 MeV (ICRU Report 26 1977). To make the sphere responses equal to Sanna's calculations in this energy range, density corrections for the spheres are performed by the LOUHI code.

Essentially, the basic equations of LOUHI solve for neutron flux, absorbed dose, average neutron energy, and dose equivalent rate. LOUHI uses equation (1) to determine neutron flux in the jth energy band, ϕ_j:

$$A_i = \sum_{j=1}^{26} R_{ij} \, \phi_j \tag{1}$$

where: A_i = the count rate with the ith detector configuration, and is obtained by integrating under the peak using a log background subtraction continuum and dividing that value by the count time for each individual detector configuration, and

R_{ij} = one of the response functions of the ith detector in the jth energy calculated by Sanna (1973), and is directly available from his tabulations.

8

The average neutron energy calculation incorporates a weighting function shown in equation (2):

$$Eav = \sum_{j=1}^{n} w_j \cdot E_j \cdot F_j \cdot F_s^{-1} \tag{2}$$

where:
Eav = average neutron energy

j = energy band (1-26)

n = total number of energy bands (26)

w_j = weighting function of jth energy band

E_j = energy value at the jth point, in MeV

F_j = the solution at point j

F_s = total flux

The dose equivalent rate equation uses a weighting function and a precalculated neutron flux-to-dose equivalent conversion ratio as shown in equation (3):

$$DS = \sum_{j=1}^{n} w_j \cdot d_j \cdot F_j \tag{3}$$

where:
DS = dose equivalent rate

d_j = neutron flux to dose equivalent conversion factor for neutrons in the jth energy band.

Flux-to-dose equivalent conversion factors are compiled as a subroutine in the LOUHI program and have been taken directly from tables in ICRP 21 (1971). Absorbed dose calculations are performed in a subroutine called Element 57 dose rate, developed at Oak Ridge National Laboratory. This model is used to estimate the dose in various regions of a homogeneous anthropomorphic phantom, which was taken as a right cylinder with a radius of 15 cm and a height of 60 cm. Composition of the phantom was assumed to be H, C, N, and O in the proportions of standard man. The cylindrical volume was divided into 150-numbered volume elements and the average dose per neutron flux in the incident beam was computed for each volume element. The neutron beam was assumed to be broad enough to irradiate the whole phantom, and to be

9

monoenergetic and monodirectional with velocity vector parallel to the
base of the cyclinder (Auxier, Snyder and Jones 1968). The maximum dose
rate, which in this scheme is to Element 57, is used for estimating depth
dose rate at the energy levels measured in reactors. Quality factors are
not directly calculated by the LOUHI unfolding code but can be easily
determined by dividing the dose equivalent rate by the Element 57 absorbed
dose rate.

Quality factor values determined by this method will not be the same
as Q values calculated by the TEPC computer program. The significance of
this point will become more apparent as it is shown that both systems
derive dose equivalent rates and Q's using different methodologies. Further
discussion of the LOUHI program is readily available in the literature
(Awschalom 1966; Bramblett, Ewing and Bonner 1960; Routti and Sandberg 1978;
Sanna 1973).

There are two additional sphere sizes that are normally associated with
the multisphere system but were not used in this study. They are the 5.08 cm
and 45.7 cm diameter spheres. The smaller of the two, the 5.08 cm sphere,
produces a response very nearly equal to that of the cadmium shielded detector.
When a hole was bored into the 5.08 cm sphere, to accommodate the detector,
a considerable amount of moderating material was removed. This loss of
moderating material introduced serious implications as to the validity of
the 5.08 cm sphere response; therefore, it was not used. In place of the
5.08 cm response a well-defined cadmium cutoff point of 0.4 eV was established
as the next to lowest energy band (the response of the bare detector being
the lowest). The larger sphere, 45.7 cm, would normally be used to provide
a response in the energy range of >3 MeV. With the prior knowledge of low
energy ranges (<1 MeV) in containment, it was determined that the larger
sphere was not needed.

To determine the amount of additional information gained by using the
25.4 and 30.5 cm diameter spheres a reanalysis of data was performed. Both
of these spheres have a similar energy response at approximately 2 MeV, which
potentially overemphasizes the spectrum in that energy range. This reanalysis
was performed using the responses from all seven detectors, responses from

all six detectors except the 30.5 cm response, and all six detector responses except the 25.4 cm response. The average energy results from the two six-detector variations were within ±12% of the results obtained with all seven-detector responses. Absorbed dose, total flux, and dose-equivalent rate results were within ±6% of the seven-detector response results. This indicates that contribution of neutrons with energies >0.7 MeV is very small inside containment. The use of both the 25.4 and 30.5 spheres do not produce a significantly different spectral response at the higher energy end of the spectrum.

A typical multisphere data table generated by the LOUHI code shows the calculated fluxes, energies, and integral dose equivalents over the 26 points with the final results compiled at the bottom of the table (see Table 1). From this data, the plots of flux versus energy were developed.

TISSUE-EQUIVALENT PROPORTIONAL COUNTER (TEPC)

While the multisphere technique requires several measurements and uses a complex computer program for unfolding, the TEPC requires but a single measurement with relatively simple analytical techniques. A block diagram of the TEPC system and instrumentation settings is shown in Figure 2. The electronic system components include detector, preamplifier, amplifier, and high voltage power supply. The multichannel analyzer (MCA) used with the TEPC has a log display which greatly assists in the analytical inter-pretation of the unanalyzed data. Figure 3 shows the multisphere, TEPC, and associated electronic systems.

The TEPC is a hollow sphere of tissue equivalent plastic (Shonka A150 muscle equivalent plastic with the walls 3.2 mm thick) filled with methane-based tissue equivalent gas. Details of plastic and gas compo-sition and methods of construction can be found in ICRU Report 26 (1977). This form of TEPC, called a Rossi Counter, has a helical grid around the central anode wire. The helical grid establishes uniform lines of force along the entire length of the anode. This produces the needed uniformity in gas amplification at all points along the anode for proper pulse height analysis. The plastic sphere is contained inside a metal pressure

11

Table 1. Multisphere Data Table

	E(I) (MeV)	Differential Flux (n/cm²-MeV-s)	Integral Flux	Integral Dose Equivalent	Energy Band (MeV)	Flux (n/cm².s)
1	2.07E-07	3.77E+08	1.00E+00	1.00E+00	3.89E-07	1.47E+02
2	5.32E-07	5.16E-07	8.03E+07	9.28E-01	2.69E-07	1.39E+01
3	9.93E-07	8.52E+06	7.85E-01	9.20E-01	7.63E-07	6.50E+00
4	2.10E-06	1.83E+06	7.76E-01	9.17E-01	1.61E-06	2.95E+00
5	4.45E-06	5.14E+05	7.72E-01	9.15E-01	3.42E-06	1.76E-00
6	9.42E-01	1.88E+05	7.70E-01	9.15E-01	7.22E-06	1.36E+00
7	2.00E-05	8.73E+04	7.68E-01	9.14E-01	1.53E-05	1.34E+00
8	4.22E-05	4.99E+04	7.66E-01	9.13E-01	3.23E-05	1.61E+00
9	8.94E-05	3.40E+04	7.64E-01	9.12E-01	6.89E-05	2.34E+00
10	1.89E-04	2.65E+04	7.61E-01	9.11E-01	1.45E-04	3.84E+00
11	4.04E-04	2.27E+04	7.55E-01	9.10E-01	3.18E-04	7.22E+00
12	8.55E-04	2.03E+04	7.46E-01	9.06E-01	6.40E-04	1.30E+01
13	1.80E-03	1.82E+04	7.28E-01	9.01E-01	1.38E-03	2.51E+01
14	3.80E-03	1.54E+04	6.985-01	8.90E-01	2.91E-03	4.48E+01
15	8.05E-03	1.17E+04	6.34E-01	8.70E-01	6.20E-03	7.25E+01
16	1.70E-02	7.64E+03	5.37E-01	8.40E-01	1.30E-02	9.93E+01
17	3.61E-02	4.04E+03	4.03E-01	7.75E-01	2.77E-02	1.12E+02
18	7.64E-02	1.65E+03	2.53E-01	6.48E-01	5.86E-02	9.67E+01
19	1.58E-01	5.00E+02	1.23E-01	4.54E-01	1.13E-01	5.56E-01
20	3.18E-01	1.10E+02	4.74E-02	2.60E-01	2.27E-01	2.50E+01
21	6.40E-01	1.75E-01	1.39E-02	1.15E-01	4.56E-01	7.89E+00
22	1.29E+00	2.12E+00	3.22E-03	3.61E-02	9.20E-01	1.95E+00
23	2.59E+00	2.05E-01	6.06E-04	7.17E-03	1.85E+00	3.79E-01
24	5.22E+00	1.68E-02	9.76E-05	1.22E-03	3.73E+00	6.27E-02
25	1.05E-01	1.23E-03	1.37E-05	1.79E-04	7.50E+00	9.23E-03
26	1.96E+01	8.56E-05	1.25E-06	1.72E-05	1.09E+01	9.33E-04

Total flux = 7.4477E+02 n/cm².s   Element 57 dose rate = 1.6681E-03 rad/hr
Dose-equivalent rate = 8.564E+00 mrem/hr   Average energy = 5.3385E-02 MeV

12

LINEAR AMP SETTINGS   MCA
COARSE GAIN 10   LOG SCALE
FINE GAIN 6.0   ZERO SETTING 2.65
SHAPING CONSTANT 1μ sec   U.L. DISCR. 10

BASE LINE RESTORER BLR   L.L DISCR. 0
  1) ASYMMETRY - x1   ACQ (ACQUIRE MODE)
  2) RATE - HIGH   DIRECT
  3) GATE - IN   OFF
UNIPOLAR OUTPUT - POSITIVE   INPUT IS IN DIRECT
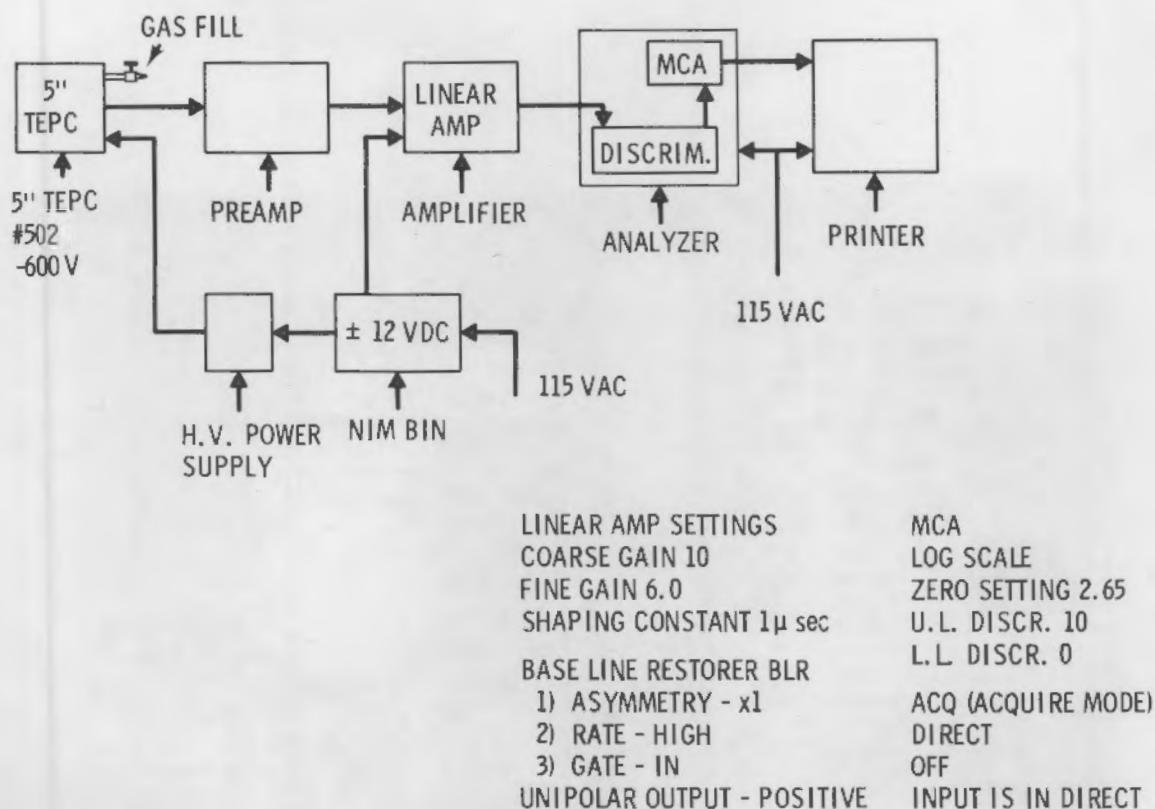
FIGURE 2. Block Diagram of the TEPC System

vessel with a valve for admitting tissue equivalent gas. The gas pressure
is maintained at a pressure of 5.6 mm Hg absolute so that charged particles
crossing the cavity lose only a small amount of energy as they transverse
the counter. Energy deposited in the cavity is then equal to the linear
energy transfer of the particle times the path length. At these low
pressures the gas-filled cavity has the same mass stopping power as a
sphere of tissue (ρ = 1 gm/cm^3) with a diameter of about one micrometer
and is said to have an "equivalent diameter" of one micrometer.

The TEPC becomes self-calibrating when the proton drop point is
identified. A proton drop point corresponds to a slow proton recoil
having the highest linear energy tranfer or stopping power traversing
the diameter of the spherical cavity and is independent on the initial
energy of the neutron producing the event. According to the data of

13

FIGURE 3.   Multisphere Spectrometer and TEPC Systems
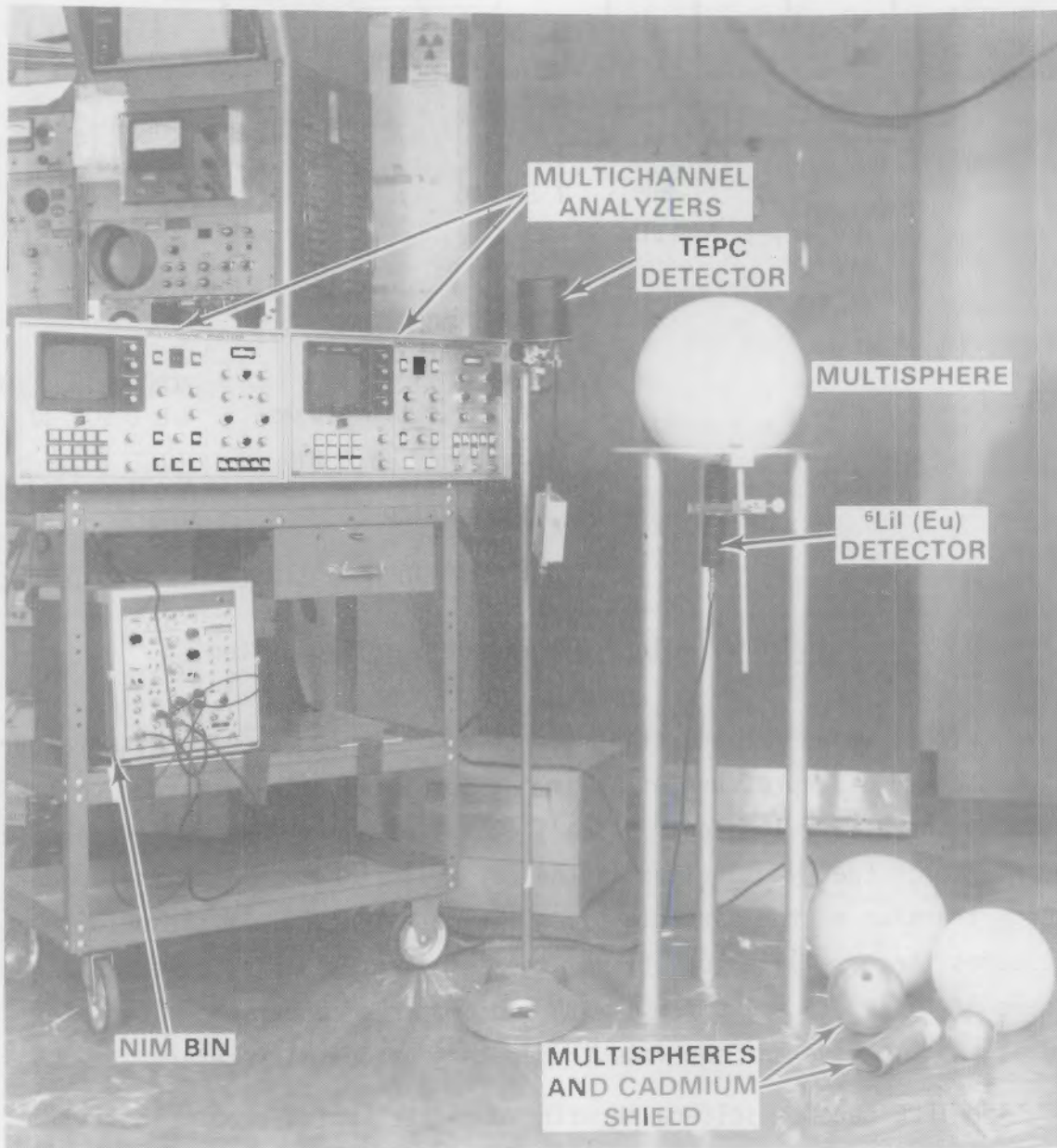
Glass and Samsky (1967), this point occurs at about 100 keV/μm and is a slowly varying function of tissue-equivalent gas pressure.

Multiplying the number of events of a given size by the energy of the event gives the absorbed energy distribution in the TE gas, which is a direct measure of absorbed dose. Following the nomenclature in ICRU 26 (1977), this is stated in equation (4):

$$D = 1.602 \times 10^{-8} \sum_{h_1}^{h_2} k \cdot h \cdot N(h) \cdot V^{-1} \cdot \rho^{-1} \qquad (4)$$

where: D = absorbed dose (rad)

h = the measured pulse height expressed as channel number

$N(h)$ = the number of pulses accumulated in channel h, h_1 and h_2 are the limits in pulse height between which the absorbed dose is to be determined.

ρ = the gas density, in gm/cm^3

V = the sensitive volume of the cavity in cm^3, and

k = the calibration relating energy to channel number which has determined from the proton drop point (keV/channel number).

For calculational purposes, h_1, the lower limit of event size, is defined as the minimum between photon and neutron induced events which occurs at an event size of about 15 keV/μm, and h_2 is the upper limit defined by the high energy recoils of the event size spectrum. The summation over $N(h)$ between h_1 and h_2, as shown in equation (4), is the total energy absorbed in the gas cavity divided by the mass of TE gas inside the sphere.

The TEPC event spectrum (Figure 4) shows the number of events per channel commonly referred to as the energy deposited per channel or event size spectrum. Also shown in Figure 4 are the three parameters needed to analyze TEPC data: h_1 (the lower limit), h_2 (the upper limit), and the proton drop point.
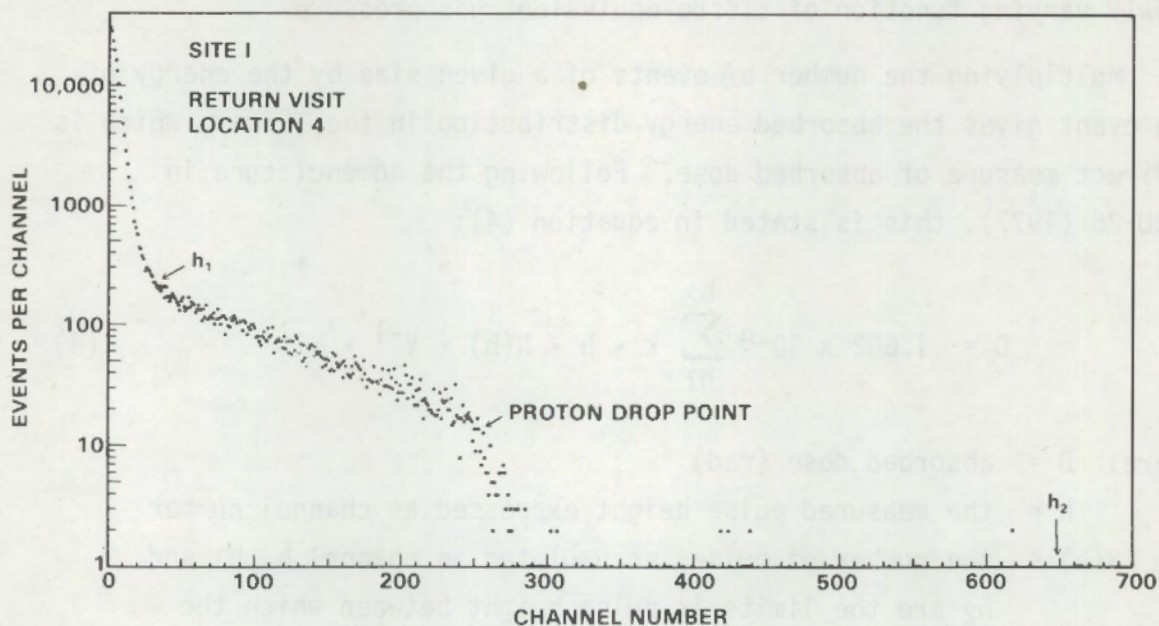
15

FIGURE 4. TEPC Event Size Spectrum

TEPC DOSE EQUIVALENT

The only general method that has been developed for the measurement
of the distribution of dose in LET is based on an analysis of the frequency
distribution of the event size due to individual particles in a spherical
volume of tissue, that is, the N(y) distribution. Actual distributions
are different from those derived with the assumptions that energy loss is
continuous and that particles travel in straight lines and have a range
that is infinitely long compared with cavity diamter. These same assump-
tions are made in the derivation of the LET spectrum from event-size
spectrum; it is evident that error is introduced. Also x-rays, electrons,
$(H(n,\gamma)D$ reactions, and positrons are assigned a Q of 1 which does not
add significantly (<0.1%) to the calculated dose equivalent. Most of these
events are below the lower limit (h_1) used in spectral analysis. However,
discrepancies between experimental and theoretical spectra are usually
sufficiently small so as to be acceptable for purposes of radiation pro-
tection. It has been Rossi's development of this technique, using the
aforementioned assumptions, that has led to a determination of dose

16

equivalent rates by calculating absorbed dose as a function of LET and by using Q as a function of LET described in ICRU 20 (1976) and ICRU 26 (1977).

H. H. Rossi devised a relatively simple model to determine the absorbed dose distribution as a function of linear energy tranfer (1968). In ICRU 26 quality factors are defined in terms of LET which makes it possible to determine dose equivalent rates and quality factors from a single TEPC measurement. The Rossi model employs a spherical counter with proton recoils arising within the walls and assumes they have a constant, uniform loss along a straight line and completely cross the cavity. Under these assumptions, the absorbed dose distributions within the cavity as a function of LET, D(L) can be calculated by equation (5) (Rossi 1968).

$$D(L) = \frac{k}{r^2} \left[y\, N(y) - y^2 \frac{dN}{dy} \right]_{y=L} \tag{5}$$

where: D(L) = absorbed dose distribution as a function of LET

k = a constant of proportionality,

r = the radius of a sphere of tissue in cm having the same mass stopping power as the tissue equivalent gas in the cavity, the lineal energy; the quotient of the mean energy imparted to the volume divided by the mean chord length in the cavity, referred to as mean event size.

N(y) = the event size distributions as a function of lineal energy, and

$\frac{dN}{dy}$ = the derivative of the event size distributions evaluated at the point where linear energy transfer and lineal energy are equal (y=L).

A computer code "TEPC" performs the above calculations by evaluating the derivative using digital filter techniques to smooth the data and computes a quality factor.

It is not possible to distinguish between photons originating from H(n,γ)D reactions in a phantom or tissue equivalent plastic counter and photons originating from external sources so all photon events below the

17

lower limit (h_1) described in equation (4) are excluded in this analysis. The Rossi model also neglects energy loss effects (energy entering and leaving the counter without being detected) from very low energy neutrons, scattering, delta rays and variations of LET along the particle track. In spite of these limitations, the Rossi model seems to be sufficiently accurate to determine quality factors within one integer value, which is adequate for health physics purposes for neutrons with energies from 200 keV to about 10 MeV. Since photon events are excluded from the quality factor analysis, this method yields a high Q for neutron energies below about 200 keV where $H(n,\gamma)D$ reactions within a phantom contribute significantly to the effective quality factor (Brackenbush, Endres, and Faust 1978).

DATA COLLECTION

Prior to making entries into containment at either reactor site, the measurement locations were determined by reviewing site specific routine surveys of the operating decks made by the plant health physicists, taking into account the capabilities and responses of the equipment as well as the potential exposure to personnel. To prevent unnecessary contamination of the equipment, it was wrapped in plastic prior to entry into radiation zones. Once inside containment, the detectors were positioned and the plastic surrounding the analyzers was opened sufficiently to prevent overheating while limiting contamination of the electronics. The analyzers, power supplies, and NIM-bin (electrical power supply rack containing high voltage power supply modules and amplifiers) were kept near the outer containment wall in the lower dose-equivalent rate areas, while the detectors, being connected to cables approximately 15 meters long, were repositioned at the end of each measurement.

The time consumed collecting data at each individual measurement location was directly dependent on the dose-equivalent rate at that location and the amount of stay time left for the personnel. To obtain more than one or two measurements at each reactor site, the total counting time per measurement location was reduced slightly, but sufficient counts were obtained in the unanalyzed spectral data for adequate computer analysis.

18

RESULTS AND DISCUSSION

RESULTS

The dose equivalent rates and neutron energy spectra observed were similar to those previously reported in the literature (Hajnal et al. 1979; Hankins and Griffith 1978). At Site F, measured dose equivalent rates in and near containment ranged from 0.3 to 5.1 mrem/hr with calculated average neutron energies ranging from 0.9 to 52 keV. The dose equivalent rates ranged from 1.5 to 3080 mrem/hr during the initial Site I visit, and the average neutron energies were 53 to 90 keV. Between Site I visits the old shielding was removed and new shielding was installed. The new shielding, which will be discussed later in this section, reduced the dose equivalent rates by a factor of 30 or more within containment, and the average neutron energies to 29 to 56 keV. With the exception of one measurement location at Site F, the major contribution to dose is from neutrons with energies >1 keV. Table 2 shows the calculated data from Site F and compares the dose equivalent rates from both TEPC and multisphere systems. Both systems were used at Locations 10 and 11 and the resultant neutron dose equivalent rates are in relatively close agreement. The TEPC was higher by factors ranging from 1.5 to 1.9 which is considered satisfactory agreement for field measurements when using two different neutron dose equivalent rate meters. Operating deck measurement locations with respect to the reactor cavities are shown in Figures 5 and 6

TABLE 2. TEPC and Multisphere Results at Site F

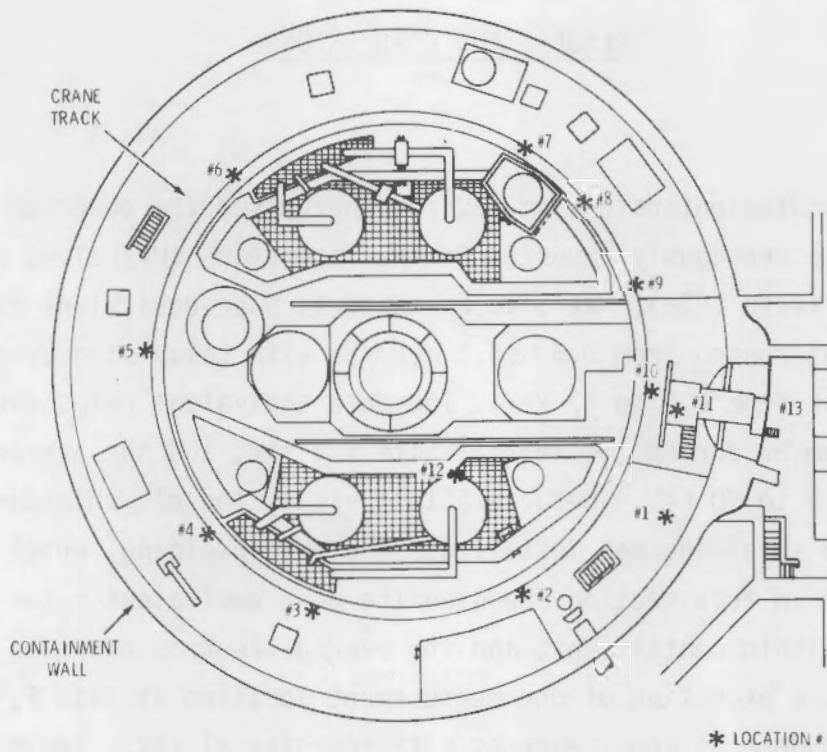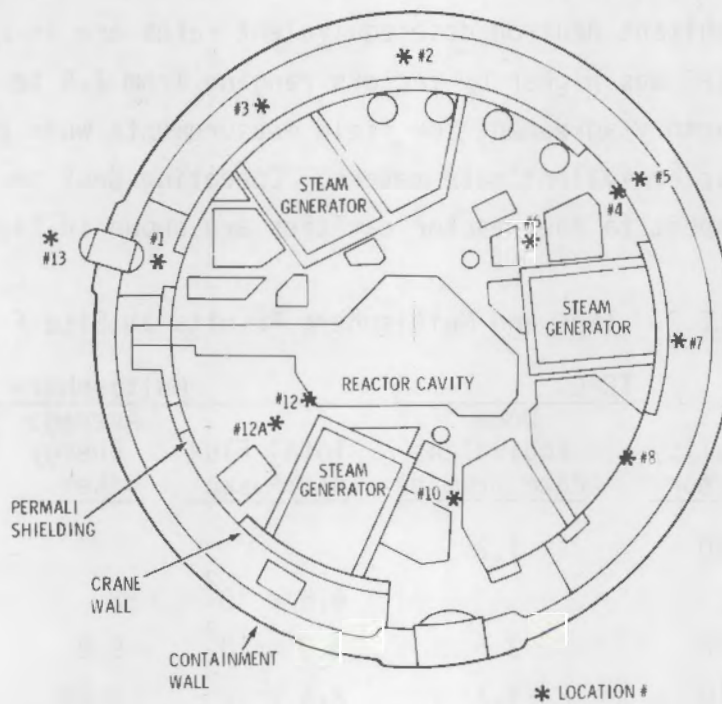| Measurement Location	TEPC		Multisphere		
	Quality Factor	Dose Equivalent Rate mrem/hr	Total Flux n/cm^2-sec	Average Energy keV	Dose Equivalent Rate mrem/hr
1	10	1.2			
5			4.5×10^2	52	5.1
10	10	3.6	4.7×10^2	9.8	2.4
11	10	1.7	2.4×10^2	0.93	0.9
13	10	0.3			

FIGURE 5. Measurement Locations at Site F

FIGURE 6. Measurement Locations at Site I

for each of these two site studies. Tables 3 and 4 show the calculated data
from the initial and return visit to Site I. Dose equivalent rates and cal-
culated average energies for the two Site I visits are compared in Table 5.

TABLE 3. TEPC and Multisphere Results at Site I (initial
visit prior to shielding modification)

	TEPC		Multisphere		
Location	Quality Factor	Dose Equivalent Rate mrem/hr	Total Flux n/cm^2-sec	Average Energy keV	Dose Equivalent Rate mrem/hr
1 Run 1	10	41	3.0 x 10	77	45
1 Run 2	10	55			
2			1.4 x 10^3	90	24
3	10	10	7.5 x 10^2	53	9
4	10	560			
5	10	290			
12	10	3080			
Middle of Airlock			1.2 x 10^2	63	1.5

TABLE 4. TEPC and Multisphere Results at Site I (second
visit after shielding modification)

	TEPC		Multisphere		
Location	Quality Factor	Dose Equivalent Rate mrem/hr	Total Flux n/cm^2-sec	Average Energy keV	Dose Equivalent Rate mrem/hr
1			8.2 x 10^1	49	0.9
4	11	16	1.4 x 10^3	56	17
7	11	3.6	4.3 x 10^2	29	3.5
8	11	29	2.1 x 10^3	49	23
12A	11	100			
13	11	0.05			

21

TABLE 5. Comparison of TEPC and Multisphere
Results Between Site I Visits

Location		Prior to Shielding Modifications			After Shielding Modifications Installed		
		TEPC mrem/hr	Multisphere mrem/hr	Average Energy keV	TEPC mrem/hr	Multisphere mrem/hr	Average Energy keV
1	Run 1	41	45	77	0.9		49
	Run 2	55					
2			24	90			
3		10	9	53			
4		560			16	17	56
5		260					
7					3.6	3.5	29
8					29	23	49
12		3080					
12A					100		
13					0.5		
Middle of Airlock			1.5	63			
Overall Average Energy				71			49

During both Site I visits the TEPC and multisphere systems produced dose
equivalent rates nearly equal with the TEPC being slightly higher in most
cases by factors ranging from 1.03 to 1.27. Only at Location 4, during the
return visit, did the multisphere system produce a higher dose equivalent
rate than the TEPC, the ratio being 1.06. Given an uncertainty of ±10% of
the multispheres (Awschalom 1966), none of the above differences is statisti-
cally significant at the 95% confidence level. Table 5 also shows the reduc-
tion in dose equivalent rates and average neutron energies after the shielding
modifications were installed. In nearly every case, the measured response
obtained with the multisphere was in close agreement with the calculated
response to within ±5% indicating a good convergence of the computer fit.

The multisphere system with the 1.27 x 1.27 cm detector determines dose
equivalent rates in the range from 0.1 mrem/hr to approximately 70 mrem/hr.
Smaller detectors can be used for higher dose equivalent rates but were not
available for this study. This limitation precluded taking multisphere mea-
surements between the crane wall and the reactor cavity. There are several
locations in which spectral information is needed, but cannot be obtained

because of high dose equivalent rates. Also, the complexity of electronics combined with the multiple responses needed for computer input makes the multisphere system awkward to use. Its most positive attribute is the ability to measure neutron energies over the entire range from thermal to several MeV.

DISCUSSION

Containments at Sites F and I have significant differences in their basic construction. These differences partially account for the lower dose equivalent rates and lower average neutron energies found at Site F. The inside diameter of the Site I containment wall is approximately four meters smaller than Site F's (16.5 m compared to 20.4m). This difference contributes to lower fluxes and reduced dose equivalent rates at or near the perimeter of the containment wall at Site F. The distance between the crane track and containment wall at Site F (see Figure 5) is nearly double the distance between the concrete crane wall and containment wall at Site I (see Figure 6). This difference is significant because the majority of personnel stay between the containment wall and the crane track or crane wall, depending on the reactor site, while they are inside containment because it is usually the lowest dose equivalent rate area.

To reduce the ^{16}N gamma (6.1 and 7.1 MeV) exposures on the operating deck, concrete walls approximate 2.44 meters tall surround the steam generators at both sites. Also, at Site F these shield walls support a small deck that places the individual another 1.8 to 2.4 meters higher in relationship to the reactor when approaching the cavity (Figure 5 shows the deck and ladder near Location 12). The reactors at both sites are at approximately the same level (approximately 7.6 meters below the operating deck in the cavity).

The reactor cavity annulus walls at both sites are made of boron loaded concrete; the annulus wall at Site F is approximately 1.22 meters thick, that is Site I is only 0.9 meters thick. The thinner shield at Site I results in increased streaming through the concrete walls upward toward personnel on the operating deck, increasing exposure rates inside the crane wall. The operating deck at Site I consists of large areas of steel grating and open unshielded areas. Perhaps the most significant difference between the two sites is in

23

the shielding placed in the annulus above the hot and cold leg inlets and outlets of the reactor. At the time the measurements were made, Site F had 61 cm of shielding consisting of lead bricks mixed with boron frit in a ratio of 3.7:1.

During the initial visit to Site I, standard borated polyethylene was wrapped around the inlet and outlet legs of the reactor vessel with no shielding in the annulus. This type of material did not appear to be providing sufficient shielding, as is indicated at measurement Location 12 (Table 3) where the neutron dose equivalent rate was >3 Rem/hr. Consequently, during an outage between Site I visits, it was replaced with a new neutron attentuating material, a silicon based elastomer with a hydrogen density of approximately 0.06 gm/cm^3 91.5% by weight). The configuration of the shields is shown in Figure 7. To obtain the elastomer and prevent it from creeping or crumbling, special containers with an outer wall of 0.95 cm thick carbon steel and inner wall of 0.02 cm stainless steel were constructed.

Another change in neutron shielding at Site I dealt with gaps in the concrete crane wall. For routine operations between major shutdowns, the crane wall openings were blocked up with a new material, Permali, Type JN. Permali is a commercially available densified beechwood laminate incorporating 6% hydrogen and 3% boron (by weight). The combined effectiveness of Permali, is reflected by the reduction in neutron dose equivalent rates by a factor of 30 to 40 at Location 1, 4, and 12A (shown in Table 5).

Figures 8, 9, and 10, flux versus energy, show only minor changes in the spectra at various locations around the perimeter of the crane wall. These changes were primarily dependent on whether the measurement was taken in a gap in the crane wall or behind the crane wall. Measurements taken in the gaps were relatively free of obstructions between the detector and the edge of the cavity. The higher flux rates detected in these areas caused the greatest amount of shifting in the intensity of the spectra while the average energies and the shape of the spectra remained relatively the same everywhere. The general lack of directional streaming and uniformity of energies at all points near the crane wall/track indicates a homogeneous spectrum that is highly moderated and scattered.
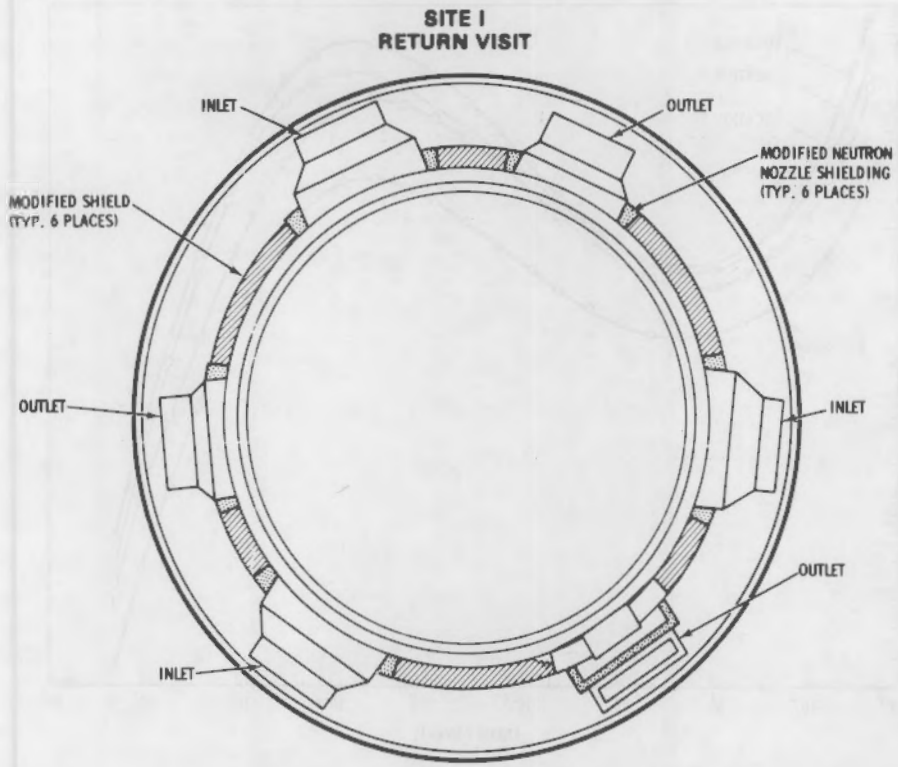
24

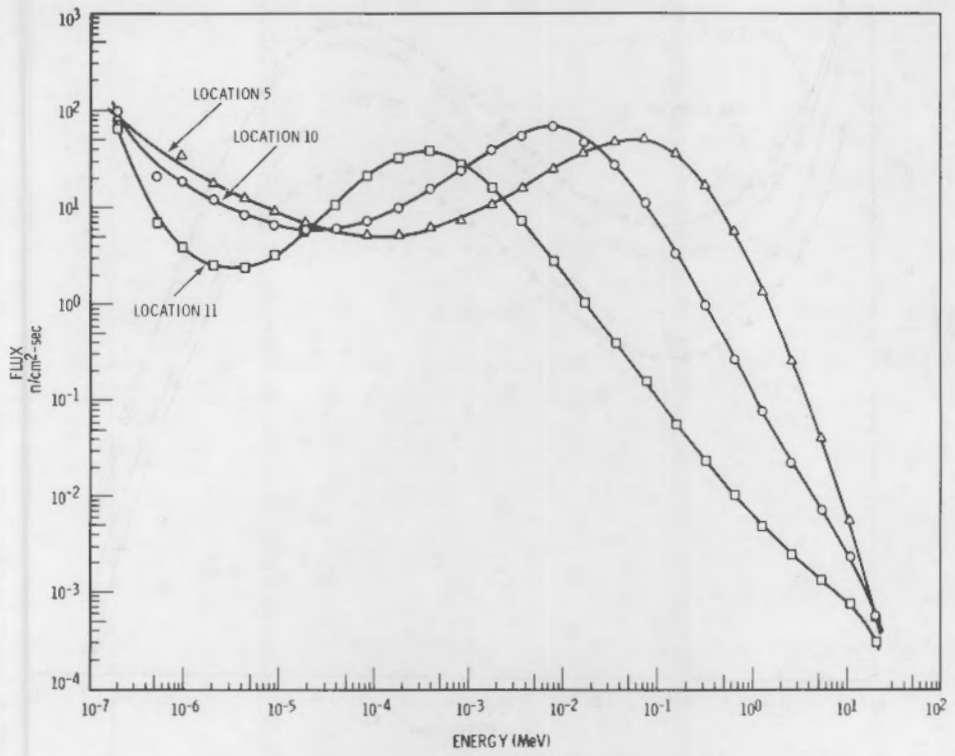FIGURE 7. Site I Silicon-Based Elastomer Shielding Modification
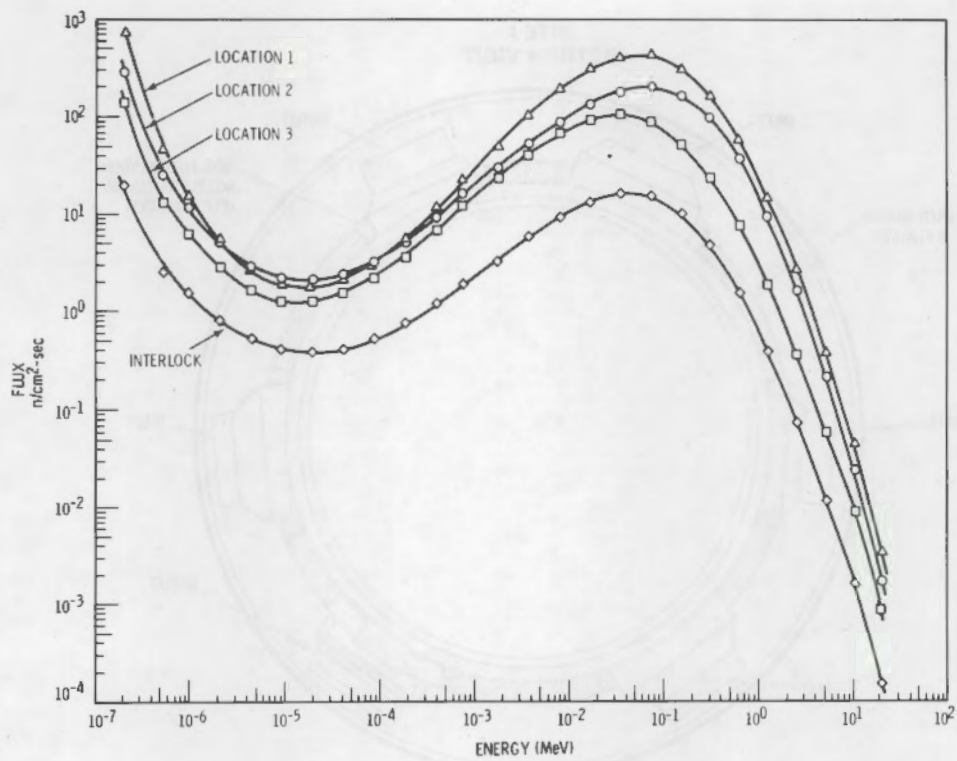

FIGURE 8. Neutron Spectra at Site F

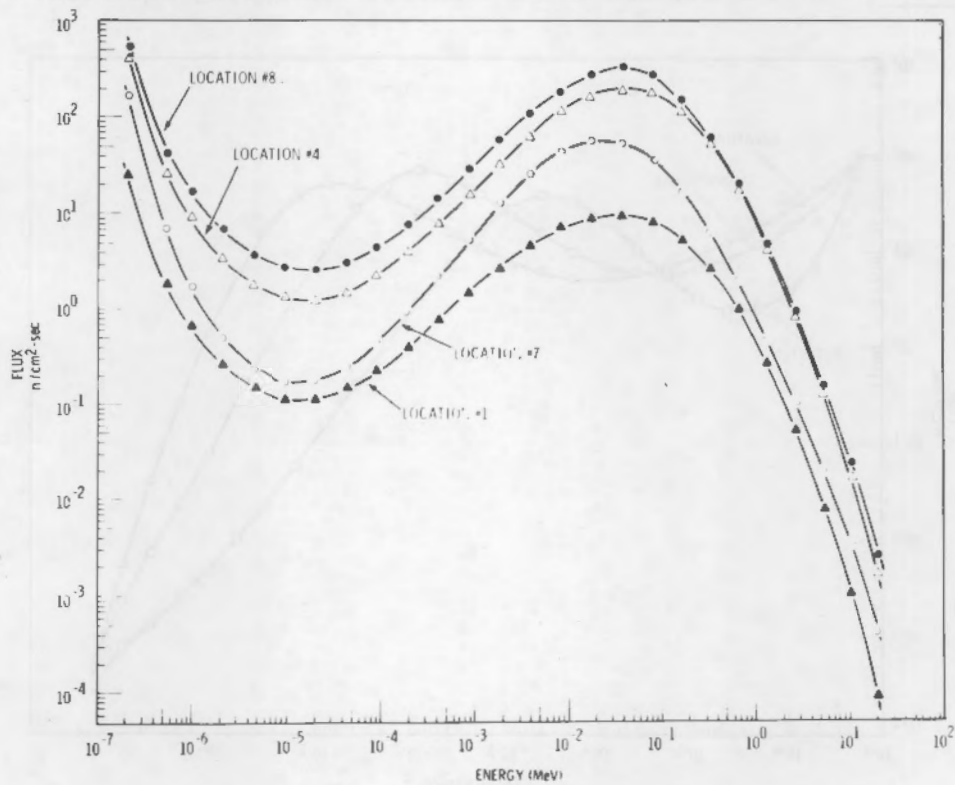**FIGURE 9.** Neutron Spectra at Site I (initial visit)

FIGURE 10. Neutron Spectra at Site I (return visit)

The initial reactor vessel shielding and the thinner annulus walls at Site I combined to produce dose equivalent rates that were relatively high (see Table 3). Working in high dose equivalent rate areas places an added stress on plant personnel performing semi-routine operations because of stay time limits. As shown earlier in Table 5. the improved shielding around the reactor vessel and nozzles at Site I produced a significant reduction in neutron dose equivalent rates.

Location 13, shown in Figures 5 and 6, is outside the airlocks with both the inner and outer doors closed. TEPC measurements at this location indicate the amount of streaming through the airlocks. Levels at this location at Site F were higher than at Site I. The reason for this difference is that at Site F there is an iron shield wall between the inner door of the airlock and the cavity whereas at Site I there is a Permali wall just inside the air-lock. Clearly, the Permali is a better shield than the iron wall from the standpoint of reducing neutron dose equivalent. Although this improvement was expected, it is important with respect to reduction in personnel exposure, long-term irradiation damage to cables, and electrical instrumentation which may be sensitive to neutrons.

CONCLUSIONS

Neutron spectra and dose equivalent rates were not constant in and
around containment as expected but, more importantly, the spectral data shows
few neutrons with energies greater than 700 keV. This finding has serious
implications for personnel neutron dosimetry and substantiates the recommen-
dation by the Nuclear Regulatory Commission to remove NTA film as a neutron
personnel dosimeter at reactors (Nuclear Regulatory Guide 8.14 1980). NTA
film is not a reliable dosimeter for use in the assessing neutron dose
equivalents when a large proportion of the neutron dose is from neutrons
with energies less than 0.7 MeV (Nuclear Regulatory Guide 8.14 1980), which
is considered the effective threshold energy of film. Track-etch neutron
dosimeters, which are based on inelastic proton recoils, are also inadequate
in this energy range.

The most widely used type of neutron personnel dosimeters sensitive to
this energy range (0-700 keV) are albedo dosimeters, but they also have an
inherent problem, that of overresponse. To make the albedo system effective
in this energy range, correction factors have to be determined. One method
by which correction factors can be determined is to use the ratio of
22.8:7.6 cm sphere responses. These ratios, when applied to a response curve,
not only give approximate neutron energies at each measurement location but
also correction factors. Hence, by applying the appropriate correction factor
to the albedo response, the dose equivalent can be determined.

The shielding change at Site I showed a significant reduction in dose
equivalent rates by a factor of 30 in most locations. The combination of
elastomer-based boron loaded silicon and Permali produced a well-moderated
neutron spectrum and a reduction in average neutron energy by a factor of
1.5. By using these new shielding materials, the thinner annulus walls and
large gaps in the operating deck floor do not create as great an exposure
problem. If the floor were solid concrete there would be an additional
benefit in the reduction of dose equivalent rates. The use of boron loaded
lead bricks in the annulus cavity, thicker annulus walls, and a solid
concrete floor at Site F provided a very well-moderated neutron spectra and

28

and very low average neutron energies. The effects of these shielding materials should be taken into consideration prior to future neutron shielding installation.

The dose equivalent rates derived by different methods compare very favorably. At the seven locations in which both instrument were used, the calculated dose equivalent rates were within ±47% of the mean of the two. At the relatively low dose equivalent rate levels in which the measurements were made, this variation is considered well within acceptable differences for operational health physics purposes. At five out of the seven measurement locations the instruments produced dose equivalent rates differing by no more than ±1.5 mrem/hr; the greatest difference was 10 mrem/hr in a field of approximately 50 mrem/hr.

The TEPC, with some miniaturization of electronics and a data input/output mechanism, could be made into a useful portable survey instrument for field use. By contrast, the multisphere system is somewhat awkward to use in that several measurements are required and manipulation of bulky moderators require additional time in high dose equivalent rate areas; hence, greater exposure to the operator. Moreover, reactor containment environments have unpleasant working conditions. Also, the detector size precludes collecting spectral data in areas of interest inside containment.

REFERENCES

Auxier, J. A., W. S. Synder and T. D. Jones. 1968. "Neutron Intersections and Penetration in Tissue." In Radiation Dosimetry, Vol. I, pp. 293-307. Ed. F. H. Attix, W. C. Roesch, and E. Tochilin. Academic Press, New York.

Awschalom, M. 1966. "Use of the Multisphere Neutron Detector for Dosimeter of Mixed Radiation Fields." In Proceedings of the Symposium on Neutron Monitoring for Radiological Protection, International Atomic Energy Agency, 29 August - 2 September 1966, Vienna, Austria.

Brackenbush, L. W., G. W. R. Endres and L. G. Faust. 1973. "Experimentally Determined Quality Factors for Fast Neutrons." BNWL-SA-4249, Pacific Northwest Laboratory, Richland, Washington.

Brackenbush, L. W., G. W. R. Endres and L. G. Faust. 1979. "Measuring Neutron Dose and Quality Factors with Tissue Equivalent Proportional Counters." In Proceedings of a Symposium on Advances in Radiation Protection Monitoring, 26-30 June 1978, Stockholm, Sweden.

Bramblett, R. L., R. I. Ewing and T. W. Bonner. 1960. "A New Type of Neutron Spectrometer." Nuclear Instruments and Methods 9, North-Holland Publishing Co., Amstersdam, Netherlands.

Glass, W. A., and D. N. Samsky. 1967. "Ionization in Thin Tissue-Like Gas Layers by Monoenergetic Protons." Radiat. Res. 32:138-148.

Griffith, R. V., and J. C. Fisher. 1976. Lawrence Livermore Laboratory Hazards Control Progress Report No. 51, July through December 1975. UCRL-50007-75-2, Lawrence Livermore National Laboratory, University of California, Livermore, California.

Griffith, R. V., D. R. Slaughter, H. W. Patterson, J. L. Beach, E. G. Frank, O. W. Rueppel and J. C. Fisher. 1977. "Multi-Technique Characterization of Neutron Fields from Moderated ^{252}Cf and ^{239}PuBe Sources." UCRL-79483, Lawrence Livermore National Laboratory, University of California, Livermore, California.

Hajnal, F., R. S. Sanna, R. M. Ryan and E. H. Donnelly. 1979. "Stray Neutron Fields Inside the Containment of PWRs. International Symposium on Occupational Radiation Exposure in Nuclear Fuel Cycle Facilities. IAEA-SM-242/24, Los Angeles, 18-22 June 1979.

Hankins, D. E., and R. V. Griffith. 1978. "A Survey of Neutrons Inside the Containment of a Pressurized Water Reactor." In Radiation Streaming in Power Reactors. ORNL/RSIC-43, Oak Ridge National Laboratory, Oak Ridge, Tennessee.

Hughes, D. E., and J. A. Harvey. 1955. Neutron Cross Section. BNL-325, 3. Brookhaven National Laboratory, Upton, New York.

International Commission of Radiological Protection (ICRP). 1971. Data for Protection Against Ionizing Radiation from External Sources: Supplement of ICRP Publication 15. ICRP Publication 21, Pergamon Press.

International Commission of Radiation Units and Measurements (ICRU). 1976. Radiation Protection Instrumentation and Its Application. ICRU Publication 20, International Commission on Radiation Units and Measurements, 7910 Woodmont Avenue, Washington, D.C.

International Commission of Radiation Units and Measurements (ICRU). 1977. Neutron Dosimetry for Biology and Medicine. ICRU Publication 26. International Commission on Radiation Units and Measurements, 7910 Woodmont Avenue, Washington, D.C.

Robkin, M. A. 1968. "An Explicit Error Calculation for Unfolding Spectra Obtained by Foil Activation." Nuclear Int. and Methods, 65:213-216.

Rossi, H. H., and C. W. Mays. 1978. "Leukemia Risk from Neutrons." Health Physics 34(4):353-360.

Rossi, H. H. 1968. Microscopic Energy Distribution in Irradiation Matter. Radiation Dosimetry, Vol. 1, eds. F. H. Attix, W. C. Roesch, and E. Tochilin, Academic Press, New York.

Routti, J. T., and J. V. Sandberg. 1978. "General Purpose Unfolding Program LOUHI 78 with Linear and Non-Linear Regularization." Report TKK-A359, Helsinki University of Technology, Department of Technical Physics, Otaniemi, Finland.

Routti, J. T. 1969. "High-Energy Neutron Spectroscopy with Activation Detectors, Incorporating New Methods for the Analysis for Ge(Li) Gamma-Ray Spectra and the solution of Fredholm Integrals Equation." ICRL-18514, (Ph.D. Thesis). Lawrence Radiation National Laboratory, University of California, Berkeley, California.

Sanna, R. S. 1973. Thirty One Group Response Matrices for the Multi-sphere Neutron Spectrometer Over the Energy Range Thermal to 400 MeV, HASL-267. U.S. Atomic Energy Commission, Health and Safety Laboratory, New York, New York.

Smith, R. C., J. N. Strode, L. W. Brackenbush, and L. G. Faust. 1978. The Tissue Equivalent Proportional Counter "Real Time" Neutron Monitor. PNL-2807, Pacific Northwest Laboratory, Richland, Washington.

U.S. Nuclear Regulatory Commission. 1980. Personnel Neutron Dosimeter. Nuclear Regulatory Guide 8.14. Washington, D.C.

Zaidins, C. S., J. B. Martin, and F. M. Edwards. 1978. "A Least-Squares Technique for Extracting Neutron Spectra from Bonner Sphere Data." Med. Phys, 5(1):42-47.

DISTRIBUTION

No. of
Copies

No. of
Copies

OFFSITE

A. A. Churm
DOE Patent Division
9800 S. Cass Avenue
Argonne, IL 6D439

25 U.S. Nuclear Regulatory
    Commission
    Division of Technical Information
      and Document Control
    7920 Norfolk Avenue
    Bethesda, MD 2D014

Frank Swanberg, Jr., Chief
Environmental Effects Research
  Branch
Division of Safeguards, Fuel
  Cycle & Environmental Research
U.S. Nuclear Regulatory Commission
Washington, DC 20555

Judy Foulke
Environmental Effects Research
  Branch
Division of Safeguards, Fuel
  Cycle & Environmental Research
U.S. Nuclear Regulatory Commission
Washington, DC 20555

Sy Block
Division of Operating Reactors
U.S. Nuclear Regulatory Commission
Washington, DC 20555

2 DOE Technical Information
    Center
   P.O. Box 62
   Oak Ridge, TN 37830

Farenc Hajnal
Department of Energy
Environmental Measurements
  Laboratory
376 Hudson Street
New York, NY 10014

James McLaughlin
Department of Energy
Environmental Measurements Lab.
376 Hudson Street
New York, NY 10014

R. V. Griffith
Lawrence Livermore National
  Laboratory
P. O. Box 808
Livermore, CA 94550

J. C. Hampton
Joint Center for Graduate Study
100 Sprout Road
Richland, WA 99352

D. Hopper
Virginia Electric & Power Company
North Anna Power Station
Mineral, VA 23117

Russell Irwin
Virginia Electric & Power Company
North Anna Power Station
Mineral, VA 23117

A. Stafford
Virginia Electric & Power Company
North Anna Power Station
Mineral, VA 23117

Frank Rescek
Zion Nuclear Station
Commonwealth Edison Company
Zion, IL 60099

No. of
Copies

<u>ONSITE</u>

20 <u>Pacific Northwest Laboratory</u>

J. M. Aldrich (5)
L. W. Brackenbush
G. W. R. Endres
L. G. Faust
W. A. Glass
G. R. Hoenes
R. L. Kathren
R. I. Scherpelz
W. E. Wilson
Technical Information (5)
Publishing Coordination (2)

NRC FORM 335 (7 77) U.S. NUCLEAR REGULATORY COMMISSION **BIBLIOGRAPHIC DATA SHEET**	**1. REPORT NUMBER** *(Assigned by DDC)* NUREG/CR-1714 PNL-3531

4. TITLE AND SUBTITLE *(Add Volume No., if appropriate)*
Neutron Spectra and Dose Equivalent Inside Nuclear
Power Reactor Containment

2. *(Leave blank)*

3. RECIPIENT'S ACCESSION NO.

7. AUTHOR(S)
J.M. Aldrich

5. DATE REPORT COMPLETED

MONTH	YEAR
April	1981

9. PERFORMING ORGANIZATION NAME AND MAILING ADDRESS *(Include Zip Code)*

Pacific Northwest Laboratory
Richland, WA 99352

DATE REPORT ISSUED

MONTH	YEAR
August	1981

6. *(Leave blank)*

8. *(Leave blank)*

12. SPONSORING ORGANIZATION NAME AND MAILING ADDRESS *(Include Zip Code)*

Division of Health, Siting and Waste Management
Office of Nuclear Regulatory Research
U.S. Nuclear Regulatory Commission
Washington, DC 20555

10. PROJECT/TASK/WORK UNIT NO.

11. CONTRACT NO.

FIN B2282

13. TYPE OF REPORT

PERIOD COVERED *(Inclusive dates)*

15 SUPPLEMENTARY NOTES

14. *(Leave blank)*

16. ABSTRACT *(200 words or less)*

This study was conducted to determine absorbed dose, dose-equivalent rates, and neutron spectra inside containment at nuclear power plants. The purpose of the study was to measure dose-equivalent rates with various commercial types of rem meters, such as the Snoopy and Rascal, and neutron absorbed dose rates with a tissue-equivalent proportional counter; determine neutron spectra using the multisphere or Bonner sphere technique and a helium-3 spectrometer;and compare several types of personnel neutron dosimeter responses such as NTA film, polycarbonates, TLD albedo, and a recently introduced proton recoil track etch dosimeter, and CR-39. These measurements were made inside containments of pressurized water reactors (PWRs) and outside containment penetrations of boiling water reactors (BWRs) operating at full power. The neutron spectral information, absorbed dose, and dose-equivalent measurements are needed for proper interpretation of instrument and personnel dosimeter responses.

17. KEY WORDS AND DOCUMENT ANALYSIS

17a. DESCRIPTORS

17b. IDENTIFIERS/OPEN-ENDED TERMS

18 AVAILABILITY STATEMENT

Unlimited

19. SECURITY CLASS *(This report)*
Unclassified

20. SECURITY CLASS *(This page)*
Unclassified

21 NO. OF PAGES

22 PRICE
S